Digest Journal of Nanomaterials and Biostructures Vol. 15, No. 2, April - June 2020, p. 593 - 599

EFFECT OF ANNEALING TEMPERATURES ON THE STRUCTURAL AND MORPHOLOGICAL PROPERTIES OF THIN $CH_3NH_3PbI_{3-x}Cl_x$ FILMS

IQBAL S. NAJI*, ABDUL-HALEEM A. RAHEEM
Physics Dept., Science College, University of Baghdad, Baghdad, Iraq

Organometal halide perovskites are promising materials for low-cost, high-efficiency solar cells. The method of perovskie layer deposition and heat treatment play an important role in determining the efficiency of perovskite solar cells. The influence of post thermal annealing of thin $CH_3NH_3PbI_{3-x}Cl_x$ films deposited by thermal evaporation technique were demonstrated regarding their structural, and morphology properties. The structural properties were studied by x-ray diffraction analysis. The diffraction peaks of the various films are observed, showing the crystallographic structural of the samples. All films before and after annealing crystallized in the orthorhombic phase of $CH_3NH_3PbI_{3-x}Cl_x$. The surface morphology of prepared films also studied by Field Emission Scanning Electron Microscope (FESEM) and Atomic Force Microscope (AFM). The first one showed that $CH_3NH_3PbI_{3-x}Cl_x$ films exhibited sparse surface coverage on the substrate, and a crake-like morphology with few isolated $MAPbI_{3-x}Cl_x$ islands of sub-micron size can be seen all over the surface. AFM measurements for all prepared films show that the average grain size and the surface roughness increases with the increase of annealing temperature.

(Received January 6, 2020; Accepted June 19, 2020)

Keywords: Organometal halide perovskites, Structural properties, Morphological properties

1. Introduction

Global energy consumption has been continually increasing with population growth and fast-paced industrial development in recent decades, which demands renewable energy sources in view of long-term sustainable development[1].Thin-film solar cells are an important technology, promising cost-competitive solar power via reduced material and fabrication costs as compared to established crystalline silicon photovoltaics, which dominates the solar panel industry but remains relatively expensive n manufacture [2,3].The necessity of cheap energy from a clean and abundant source has naturally stirred a large research effort to find low cost and high efficiency devices to convert sunlight to electricity [4].A range of solution processed organic and hybrid organic-inorganic solar cells, such as dye-sensitized solar cells (DSC) and bulk heterojunction organic solar cells, have been intensely developed in the last two decades, but the conversion efficiencies required to compete in the energy market have not yet been realized [5].Recently, Organic–inorganic metal halide perovskite solar cells have attractive a great deal of attention because of their excellent photovoltaic performance obtainable via a facile and cheap process [6]. The organic-inorganic perovskites used for photovoltaics (PV) have an AMX_3 formula that comprises a monovalent cation, A [cesium Cs^+, Methylammonium (MA) $CH_3NH_3^+$, or formamidinium (FA)$CH_3(NH_2)_2^+$]; a divalent metal, M (Pb^{2+} or Sn^{2+});and an anion, X (Cl^-, Br^-, or I^-) [7]. Organic-inorganic perovskite materials have received much interest for scientific study and device application due to their unique optical, electronic, magnetic properties, and facile film processing [8]. It have achieved certified power conversion efficiencies of 22.1% [7].The reason for the rapid increase in power conversion efficiency (PCE) of such devices is that perovskite materials have optimal properties enabling use as a light harvester in a solar cell, including direct band gap, high absorption coefficient, and excellent carrier transport[9-11].

* Corresponding author: moonbb_moonaaaa@yahoo.com

Organolead trihalide perovskites are emerging as the most attractive materials in solution-processed, low cost photovoltaic devices, which has high power conversion efficiencies (PCEs) Besides strong light absorption coefficient throughout UV-Vis-NIR spectrum, organolead trihalide perovskites (i.e. $CH_3NH_3PbX_3$) have some outstanding optoelectronic properties, such as high carrier mobility, long charge diffusion length(1μm), which is several orders longer than other emerging semiconductors, and charge-carrier lifetime, bipolar transport and so on [12,13].

$CH_3NH_3PbI_3$ has attracted increasing attentions and makes extremely fast progress in photovoltaic applications, Since their first use as sensitizing materials in 2009 by Kojima et al.[14]. One of the remarkable features of $CH_3NH_3PbI_3$ solar cells is the low carrier recombination at their interfaces; by simply introducing the perovskite-light-absorber layer between electron and hole transport layers, a high short circuit current density (Jsc) of approximately 20 mA/cm^2can be obtained with an internal quantum efficiency (IQE)of (90–100)% [15].

The incorporation of chloride with $CH_3NH_3PbI_3$ improves the uniformity of its layer [16], risen carriers mobility and diffusion length from 100 nm to over 1μm, as well as carriers transport at interface [13,17].

Therefore, one of the main challenges is the fabrication of high-quality films with controlled morphology, high surface coverage and minimum pinhole formation for high performance in perovskite devices [9].

In this work, the change in structural, and morphological properties with post heat treatment of the $CH_3NH_3PbI_{3-x}Cl_x$ films deposited by thermal evaporation method has been studied.

2. Experimental procedures

$CH_3NH_3PbI_{3-x}Cl_x$ solution received from Ossila Limited, Kroto Innovation Centre Broad Lane, UK, which mixtures of N,N-Dimethyl formamide (DMF), Lead dichloride ($PbCl_2$), and methylammonium iodide (MAI) with concentration <80%,40%,40%, respectively. Thin films of this material were prepared by thermal evaporation technique on glass substrates with rate equal to 6.6 nm/min. Before vacuum deposition, the substrates were ultrasonically cleaned in sequence by detergent, deionizer water, methanol for 15min subsequently, substrates were fixed on a sample holder and transferred into the vacuum chamber (Bulzer), and the boat was heated as the base pressure reached to $2x10^{-5}$ mbar. After finishing deposition, thin films were thermally annealed in vacuum for 30 min at different annealing temperatures (100, 150, 200^oC).

The microstructure of samples were recorded using x-ray powder diffractometer with CuKά (λ=1.5418A, 30 kV, 30 mA) model (Bruker, Germany) in a range of 2θ= 20^o-80^o at scanning rate 1 min^{-1}. The surface morphology of sample is studied by investigation of Atomic Force Microscopy (AFM) (AA3000 Scanning probe microscope, Angstron Advanced Inc.).The difference in the shape of the perovskite crystals studied by images of field emission Scanning Electron Microscope (FE-SEM) (Hitachi S-4700 field emission microscope), analysis is performed by using a magnification 10kx and 70kx, SEM in secondary electron mode.

3. Results and discussion

To investigate the structural evaluation of $CH_3NH_3PbI_{3-x}Cl_x$ thin films prepared by thermal evaporation technique before and after annealing for 30min at temperatures equal to 100 and 200 °C were recorded. The XRD pattern are shown in Fig. 1. The diffraction peaks of the various films are observed, showing the crystallographic structural of the samples. All films before and after annealing crystallized in the orthorhombic phase of $CH_3NH_3PbI_{3-x}Cl_x$.

The XRD pattern of as-deposited $CH_3NH_3PbI_{3-x}Cl_x$ film shows single phase (orthorhombic phase) which have main diffraction peaks at 2θ positions 14.06, 28.28 and 31.75^o were assigned to the (110), (220) and (310) diffraction planes of $MAPbI_{3-x}Cl_x$ with very small peak appears at 12.53^{o}can be indexed to the (001) planes of PbI_2, as shown in Fig.1a.This result agree with Chen et al. and Chuang et al. [18,19] . While XRD Pattern of the heat treated $MAPbI_{3-x}Cl_x$ film at 100°C revealed a marked increases in intensity of perovskite peaks, also notably ,looking closely at the region of the (110) diffraction peak at 14.06^o , there is a small signal of diffraction peak at 12.53^o (the (001) peak for pbI_2) under ambient conditions as shown in Fig.1b. It is worth noting here that the presence of such phase is excepted to reduce the concentration of Pb ions available for

perovskite formation, which could be expected to negatively affect the solar cell performances [20]. There is no measurable diffraction peak at 15.5° corresponding to (100) planes of the single phase of cubic $CH_3NH_3PbCl_3$ [21], manifesting a high level of phase purity of $CH_3NH_3PbI_{3-x}Cl_x$ films by the annealing temperature of 100°C.

Almost of peaks related to the perovskite layer disappeared in the diffraction pattern during thermal annealing at 200°C (Fig.1c), just the peak of (220) plane appeared with low intensity. On the basis of these finding, Tania et al.[22] concluded that the perovskite layer degraded in to pbI_2 in less than 10h . Similarly, Philippe and co-workers investigated the effect of higher temperature on both $MApbI_3$ and $MApbI_{3-x}Cl_x$ films [23], they used hard x-ray photoelectron spectroscopy (HX-PES) instead of XRD.

Also very small peaks appeared at 15.398° and 56.375° corresponding to the (100) and (223) planes of single-phase of cubic $CH_3NH_3PbCl_3$ and orthorhombic phase of $PbCl_2$, respectively. $CH_3NH_3PbCl_3$ is not suitable for the absorber layer of efficient PSCs due to its significantly higher energy band gap than that required to achieve the Shockley Queisser limit [24].

The d-spacing was calculated from Bragg law and the crystallite sizes of $MAPbI_{3-x}Cl_x$ films were estimated by using Scherrer formula, where the crystallite sizes for (110) peak of as deposited film was 19.24 nm and increases to 23.55 nm when film annealed at 100°C,All structure parameters are listed in Table 1.

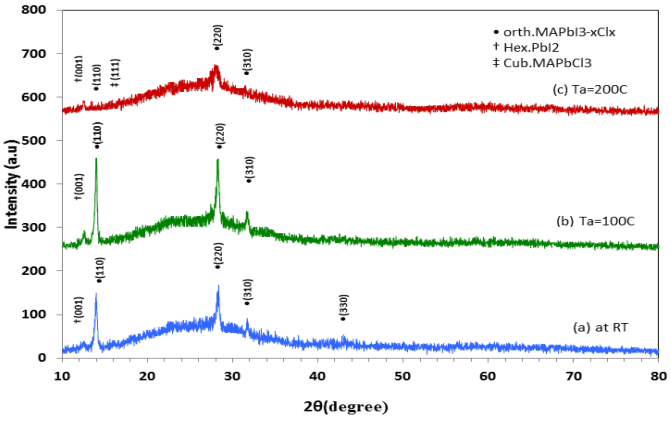

Fig. 1. The XRD pattern for as-deposited and annealed $MAPbI_{3-x}Cl_x$ thin films.

Table 1. The structural parameters of as-deposited and annealed $MAPbI_{3-x}Cl_x$ thin films.

T_a(°C)	2θ(deg.) (exp.)	2θ(deg.) (theor.)	d_{hkl}(nm) (exp.)	d_{hkl}(nm) (theor.)	I/I_o	hkl	FWHM (deg.)	C.S (nm)	Phase
R.T	12.5440	12.53	7.05089	7.058	13	001	0.008378	16.64	Hex.PbI_2
	14.0260	13.99	6.30905	6.324	100	110	0.007261	19.24	Orth.$MAPbI_{3-x}Cl_x$
	28.2872	28.36	3.15241	3.144	78	220	0.008669	16.49	Orth.$MAPbI_{3-x}Cl_x$
	31.7512	31.51	2.81594	2.836	23	310	0.005236	27.53	Orth.$MAPbI_{3-x}Cl_x$
	43.1118	43.10	2.09657	2.096	13	330	0.006981	21.35	Orth.$MAPbI_{3-x}Cl_x$
100 °C	12.6485	12.53	6.99287	7.058	13	001	0.008378	21.60	Hex.PbI_2
	14.0336	13.99	6.30565	6.324	100	110	0.007261	23.55	Orth.$MAPbI_{3-x}Cl_x$
	28.2690	28.36	3.15440	3.144	77	220	0.008669	20.83	Orth.$MAPbI_{3-x}Cl_x$
	31.7079	31.51	2.81969	2.836	21	310	0.005236	24.77	Orth.$MAPbI_{3-x}Cl_x$
200 °C	12.5241	12.53	7.06205	7.058	28	001	0.008378	15.37	Hex.PbI_2
	14.1476	13.99	6.25509	6.324	6	110	0.007261	133.41	Orth.$MAPbI_{3-x}Cl_x$
	15.3988	15.50	5.74955	5.711	9	100	0.000873	160.32	Cubic $MAPbCl_3$
	28.0410	28.36	3.17952	3.144	100	220	0.015184	9.41	Orth.$MAPbI_{3-x}Cl_x$
	31.3717	31.51	2.84914	2.836	19	310	0.005934	24.26	Orth.$MAPbI_{3-x}Cl_x$

3.1. Atomic Force Microscope (AFM):

The surface morphology of $CH_3NH_3PbI_{3-x}Cl_x$ films prepared by thermal evaporated technique at room temperature and at different annealing temperatures (100 and 200°C) was investigated by Atomic Force Microscope (AFM).

Fig. 2 shows the AFM images, in 2D and 3D dimensions of as-deposited and annealed $CH_3NH_3PbI_{3-x}Cl_x$ at 100 and 200°C. The morphology of the as-deposited $CH_3NH_3PbI_{3-x}Cl_x$ film shows a large number of small size grains with a roughness average of 8.1 nm. However, when the sample was thermally treated at 100 and 200°C the roughness becomes 6.46 and 34 nm respectively. The surface became rougher as the annealing temperature increased to 200°C. It is known that the higher roughness sample is better for photovoltaic applications because when the surface is rough, the total surface area is much higher than the sample with low roughness. The grains diameter increased with increasing the annealing temperature. All parameters are listed in Table 2.

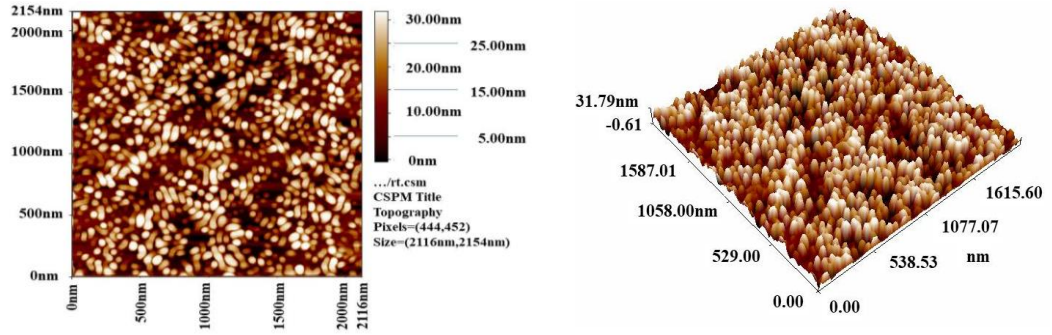

a)

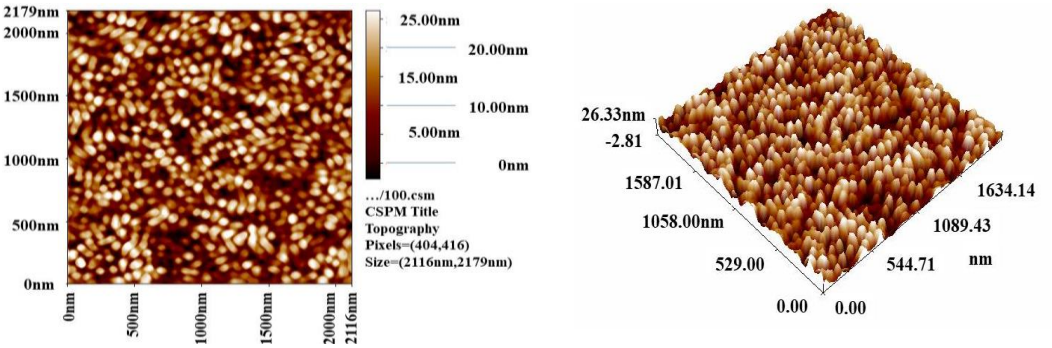

b)

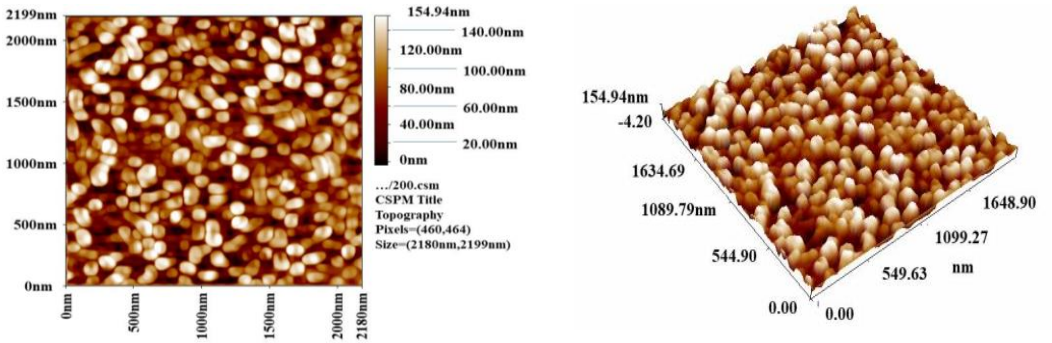

c)

Fig. 2. AFM images of thermal evaporated of (a) as deposited and annealed $CH_3NH_3PbI_{3-x}Cl_x$ thin films at (b)100C and (c) 200C.

Table 2. Average diameter, Roughness average and root mean square (nm) of deposited and annealed $CH_3NH_3PbI_{3-x}Cl_x$ thin films.

T_a (°C)	Average Diameter (nm)	Roughness average (nm)	Root mean square (nm)	Peak-peak (nm)
R.T	52.74	8.10	9.35	9.35
100	77.20	6.46	7.57	7.57
200	78.21	34.0	40.2	40.2

3.2. Field Emission Scanning Electron Microscope analysis (FESEM)

Scanning electron microscopy (SEM) is a convenient method to study the surface morphology of $MAPbI_{3-x}Cl_x$. Surface morphology of material plays an important role in solar energy conversion efficiency of the device. To achieve an efficient charge transfer and charge transport, the film morphology should be of good quality. It should be likely free from pinholes, kinks.

Top views of $MAPbI_{3-x}Cl_x$ layer deposited on glass substrate at room temperature by thermal evaporation method with different magnification are shown in Fig. 3. The film exhibited sparse surface coverage on the glass substrate, and a crake-like morphology with few isolated $MAPbI_{3-x}Cl_x$ islands of sub-micron size (grain size is around less 500nm) can be clearly seen all over the surface. However, the surface coverage is one of the most crucial factors that dominate the performance of devices, and an efficient PSC can be attained only with high surface coverage [25]. The incomplete surface coverage of perovskite not only decreases the harvest of light by passing straight though the device, but also brings a lot of pinholes as shunt paths for the direct contacts of the HTM and electron transporting layer (ETL). All these cause simultaneous drops in the short-circuit current (J_{sc}), open-circuit voltage (V_{oc}), fill factor (FF) and the corresponding PCE.

To observe the thickness homogeneity of the perovskite layer, the cross sectional SEM was performed for $MAPbI_{3-x}Cl_x$ film as shown in Fig. 4.

It is clear the average thickness of the perovskite layer seems to be uniform with thickness equals to 200 nm. The presence of the random structures on the surface (rough features on top of the perovskite layer) increases the possibility of the current leakage occurring through piercing of the ETL layer to the cathode [26].

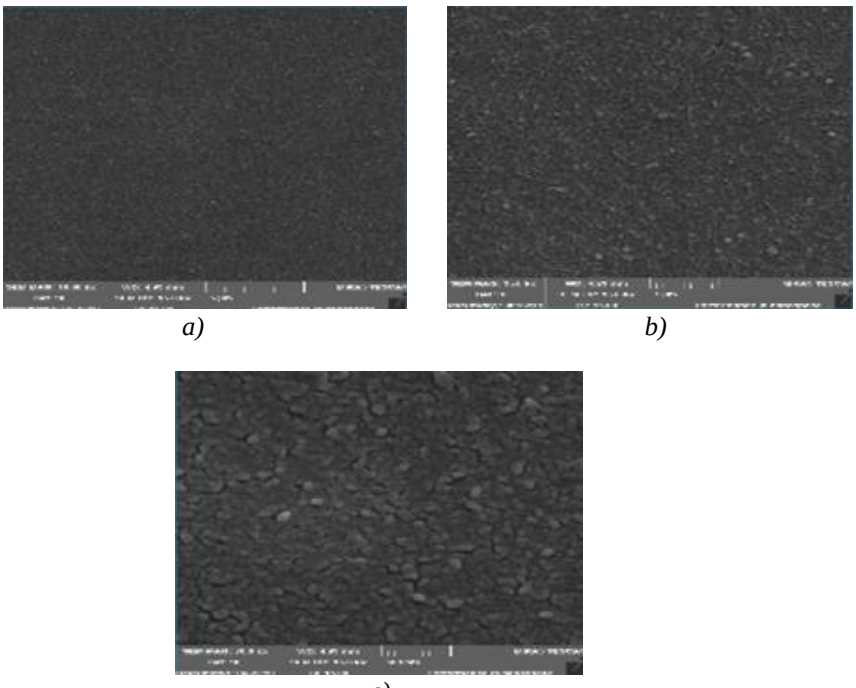

a) *b)*

c)

Fig. 3.Field emission scanning electron microscopy (FE-SEM) images of $MAPbI_{3-x}Cl_x$ at room temperature with different magnification: a)10.0 kx b) 35.0 kx c)70.0 kx.

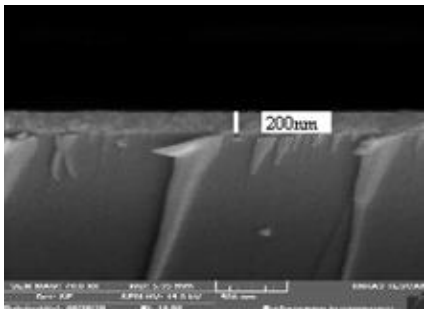

Fig. 4.Cross-sectional FESEM images of $MAPbI_{3-x}Cl_x$.

4. Conclusions

The $CH_3NH_3PbI_{3-x}Cl_x$ perovskite films deposited by thermal evaporation method had been investigated to found the optimization annealing temperature for using in solar cells applications. The improvement in the crystal structure had been achieved after annealing at 100^{o}C.

The most dominant diffraction peaks were disappeared and unwanted phases like $MAPbCl_3$ formed when the film annealed at 200^{o}C. The grain size of $CH_3NH_3PbI_{3-x}Cl_x$ film becomes greater as the annealing temperature increased. The film exhibited sparse surface coverage on the glass substrate, where the surface coverage is one of the most crucial factors that dominate the performance of devices.

References

[1] Mahdi Hasan Suhail, Aqel Mashot Jafar, Elixir Renewable Energy **98**, 42709 (2016).
[2] G. E. Eperon, V. M. Burlakov, P. Docampo, A. Goriely, Henry J. Snaith, Adv. Funct. Mater. **24**(1), 151 (2013).
[3] Nam Joong Jeon, Jun Hong Noh, Young Chan Kim, Woon Seok Yang, Seungchan Ryu, Sang Il Seok, Nature Materials **13**, 897 (2014).
[4] M. Gratzel, R. A. J. Janssen, D. B. Mitzi, E. H. Sargent, Nature **488**(7411), 304 (2012).
[5] V. Gonzalez-Pedro, E. J. Juarez-Perez, W. S.Arsyad, E. M. Barea, F. Fabregat-Santiago, I. Mora-Sero, J. Bisquert, Nano Lett. **14**, 888 (2014).
[6] Jeong-Hyeok Im, In-Hyuk Jang, Norman Pellet, Michael Grätze, Nam-Gyu Park, Nature Nanotechnology **9**(11), 927 (2014).
[7] M. Saliba,T. Matsui, K. Domanski, Ji-Youn Seo, A. Ummadisingu, S. M. Zakeeruddin, Juan-Pablo Correa-Baena, W. R. Tress, A. Abate, A. Hagfeldt, M. Grätze, Sciencemag. Org. **354**(6309), 206 (2016).
[8] D. B. Mitzi, Prog. Inor. Chem. **48**, 1 (2007).
[9] Z. R. Pratiwi, L. Nuraeni, A. H. Aimon, F. Iskandar, IOP Conf. Series: Materials Science and Engineering **395**, 1 (2018) .
[10] Sigalit Aharon, Bat El Cohen, LiozEtgar, J. Phys. Chem. C **118**(30), 17160 (2014).
[11] W. Ke, G. Fang, Q. Liu, L. Xiong, P. Qin, H. Tao, J. Wang, H. Lei, B. Li, J. Wan, G. Yang, Y. Yan, J. Am. Chem. Soc. **137**, 6730 (2015).
[12] Y. Xu,L. Zhu, J. Shi, S. Lv, X. Xu, J. Xiao, J. Dong, H. Wu, Y. Luo, D. Li, Q. Meng, ACS Appl. Mater. Interfaces **7**(4), 1 (2015).
[13] Deying Luo, Leiming Yu, Hai Wang, TaoyuZou, Li Luo, Zhu Lu, Zhenghong Lu, RSC Advances **104**, 1 (2015).
[14] Wei Geng, Chuan-Jia Tong, Zhen-Kun Tang, ChiYung Yam, Yan-Ning Zhang, Woon-Ming Lau, Li-Min Liu, Journal of Materiomics **1**, 213 (2015).
[15] M. Shirayama, H. Kadowaki, T. Miyadera, T. Sugita, M. Tamakoshi, M. Kato, T. Fujiseki, D. Murata, S. Hara, Takurou N. Murakami, S. Fujimoto, M. Chikamatsu, H. Fujiwara,

Physical Review Applied **5**(014012), 1 (2016).
[16] A. Dualeh, N. Tétreault, T. Moehl, P. Gao, M. K. Nazeeruddin, M. Grätzel, Adv. Funct. Mater. **24**, 3250 (2014).
[17] S. D. Stranks, G. E. Eperon, G. Grancini, C. Menelaou, M. J. P. Alcocer, T. Leijtens, L. M. Herz, A. Petrozza, H. J. Snaith, Science **342**, 341 (2013).
[18] Dan Chen, Xiaoping Zou, Hong Yang, Ningning Zhang, Wenbin Jin, Xiao Bai, Ying Yang, International Journal of Photoenergy **2017**, 1 (2017).
[19] Pei-Yu Chuang, Ching-Nan Chuang, Chung-Chiang Yu, Lee-Yih Wang , Kuo-Hung Hsieh, Polymer **97**, 196 (2016).
[20] Silvia Colella, E. Mosconi, P. Fedeli, A. Listorti, F. Gazza, F. Orlandi, P. Ferro,T. Besagni, A. Rizzo, G. Calestani, G. Gigli, F. De Angelis, R. Mosca, Chem. Mater. **25**(22), 4613 (2013).
[21] N. Kitazawa, Y. Watanabe, Y. Nakamura, Journal of Materials Science **37**(17), 3585 (2002).
[22] Tanzila Tasnim Ava, Abdullah Al Mamun, Sylvain Marsillac, Gon amkoong, Appl. Sci. **9**(188), 1 (2019).
[23] B. Philippe, B. W. Park, R. Lindblad, J. Oscarsson, S. Ahmadi, E. M. Johansson, H. Rensmo, Chem. Mater. **27**, 1720 (2015).
[24] Y.-C. Chern, Y.-C. Chen, H.-R. Wu, H. W. Zan, H. F. Meng, S. F. Horng, Organic Electronics **38**, 362 (2016).
[25] G. E. Eperon, V. M. Burlakov, P. Docampo, A. Goriely H. J. Snaith, Adv. Funct. Mater. **24**, 151 (2014).
[26] Neeti Tripathi, Masatoshi Yanagida, Yasuhiro Shirai, Takuya Masuda, Liyuan Han, Kenjiro Miyano, Journal of Materials chemistry A **22**, 1 (2015).